European Journal of Chemistry

Synthesis, spectroscopic, thermal and anti-microbial studies of transition metal complexes of hydrazone derived from 4,6-diacetylresorcinol and S-methyldithiocarbazate

Adel Abbas Ahmed Emara [1,2,*], Ali Mahmoud Taha [1], Mahmood Mohamed Mashaly [1] and Omima Mohamed Ibrahim Adly [1]

[1] *Department of Chemistry, Faculty of Education, Ain Shams University, Roxy, Cairo, 11711, Egypt*
[2] *Department of Chemistry, University College in Makkah, Umm Al-Qura University, Makkah, 21955, Kingdom of Saudi Arabia*

* Corresponding author at: Department of Chemistry, University College in Makkah, Umm Al-Qura University, Makkah, 21955, Kingdom of Saudi Arabia
Tel.: +966.540.551982. Fax: +966.12.5586531. E-mail address: adelaaemara@yahoo.com (A.A.A. Emara).

ARTICLE INFORMATION

ABSTRACT

New series of copper(II), nickel(II), cobalt(II), zinc(II), cadmium(II), iron(III) and oxovanadium(IV) complexes of hydrazone, H_3L, ligand derived from the condensation of *S*-methyldithiocarbazate and 4,6-diacetylresorcinol, in the molar ratio 1:1, has been synthesized. All the metal complexes are dimmers. The structures of the ligand and its transition metal complexes were characterized by elemental analyses, spectral (Infrared, electronic, Mass, ^{1}H NMR and ESR) data and magnetic susceptibility, molar conductivity measurements and thermal gravimetric analysis. The structure of the ligand is dibasic tridentate with ONS sites. The bonding sites, in all cases, are the azomethine nitrogen, phenolic oxygen and thiol sulfur atoms, as illustrated from the spectral data. The metal complexes exhibit different geometrical arrangements such as square planar, tetrahedral, square pyramidal and octahedral arrangements. Kinetic parameters (ΔG, ΔH, ΔS and ΔE) of the metal complexes were calculated from the thermal behaviour of the metal complexes using Coats-Redfern method. The ligand and its metal complexes were screened for its antimicrobial activity against *Staphylococcus aureus* and *Staphylococcus pyogenes* as Gram-positive bacteria, *Pseudomonas phaseolicola* and *Pseudomonas fluorescens* as Gram-negative bacteria and the fungi *Fusarium oxysporum* and *Aspergillus fumigatus*.

1. Introduction

Thiosemicarbazones of *S*-alkyldithiocarbazate are one of the most important classes of ligands, which have considerable pharmacological interest due to significant biological activities [1-6]. These compounds have received much attention and interest for further study because they provide an interesting series of ligands whose properties can be greatly modified by introducing different organic substituents, thereby causing a variation in the ultimate donor properties [7]. The presence of hard nitrogen and soft sulfur donor atoms in the backbones of these ligands enable them to react readily with transition metal ions yielding colored stable metal complexes [8-12]. Moreover, these complexes are potentially biologically active and exhibit antifungal, antimicrobial, antimalarial, antitumoral, antiviral, and antioxidant activities [13-20].

In this manuscript, condensation of *S*-methyldithio carbazate with 4,6-diacetylresorcinol, in the molar ratio 1:1, afforded the corresponding *S*-methyl-2-[1-(5-acetyl-2,4-di hydroxyphenyl)ethylidene]hydrazine carbodithiozate, H_3L, ligand. The reactions of H_3L ligand with transition metal ions
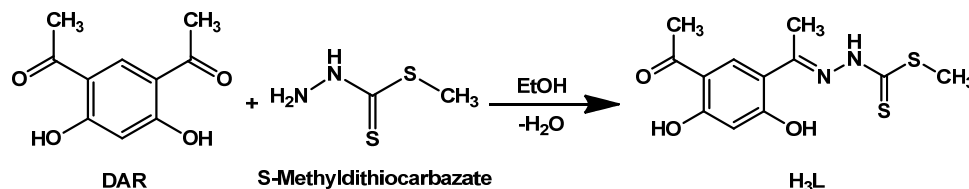
in the molar ratio (ligand:metal ion; 1:1) were studied. The newly prepared metal complexes of this ligand were identified by different physicochemical and spectroscopic techniques. Kinetic parameters (ΔG, ΔH, ΔS and ΔE) of the metal complexes were calculated from the thermal behavior of the metal complexes using Coats-Redfern method.

The ligand and its metal complexes were tested against *Staphylococcus aureus* (ATCC 25923) and *Staphylococcus pyogenes* (ATCC 19615) as Gram-positive bacteria, *Pseudomonas phaseolicola* (GSPB 2828) and *Pseudomonas fluorescens* (S 97) as Gram-negative bacteria and the fungi *Fusarium oxysporum* and *Aspergillus fumigatus*.

2. Experimental

2.1. Materials

S-methyldithiocarbazate [21] and 4,6-diacetylresorcinol [22,23] were prepared as cited in the literature. Copper(II), nickel(II), cobalt(II), zinc(II), cadmium(II) and iron(III) were used as nitrate salts and were Merck or BDH.

Scheme 1

Oxovanadium(IV) sulphate monohydrate was BDH. Lithium hydroxide monohydrate was BDH. Organic solvents [Ethanol, methanol, diethylether, acetone, dimethylformamide (DMF) and dimethylsulfoxide (DMSO)] were reagent grade.

2.2. Synthesis of H₃L ligand

The H₃L ligand was synthesized by the condensation of *S*-methyldithiocarbazate (1.22 g, 10.0 mmol) dissolved in hot absolute ethanol (30 mL) with 4,6-diacetylresorcinol (1.94 g, 10.0 mmol) in absolute ethanol (30 mL). The reaction mixture was heated to reflux for 30 min. The yellow crystals were obtained after cooling the reaction mixture to room temperature. The product was filtered off and washed with few portions of ethanol then diethylether and air-dried. Fine crystals were obtained by recrystallization from ethanol. The ligand was kept in a desiccator until used. The yield was 1.75 g (59 %) and the melting point (M.p.) was 226-227 °C. Scheme 1 illustrates the formation of the H₃L ligand.

2.3. Synthesis of the metal complexes

Methanolic solutions of the metal salts (30 mL) were added gradually to methanolic solutions of the deprotonated ligand (30 mL) in the molar ratio 1:1. In each case, the ligand was deprotonated using lithium hydroxide, LiOH.H₂O, as deprotonating agent. The reaction mixture of the deprotonated, H₃L, ligand with metal salts was heated to reflux for one to three hours. The time of the reflux depends on the formation of the solid products. The resulting precipitates were filtered off, washed with methanol then ether.

Lithium hydroxide, LiOH.H₂O (0.378 g, 9.0 mmol) dissolved in methanol (20 mL) was added to the H₃L ligand (0.894 g, 3.0 mmol) in methanol (30 mL), *i.e.*, in the molar ratio 3:1 (LiOH.H₂O:ligand) and heated to reflux for 30 min. The appropriate weight (3.0 mmol) of the metal salts was added to the ionic deprotonated ligand to form the metal complexes. The following detailed preparations are given as examples and the other complexes were obtained similarly.

2.3.1. Reaction of nickel(II) with H₃L ligand

Nickel(II) nitrate hexahydrate, Ni(NO₃)₂.6H₂O, (0.870 g, 3.0 mmol) in methanol (30 mL) was added gradually with constant stirring to a solution of the deprotonated, H₃L, ligand (0.894 g, 3.0 mmol) in methanol (30 mL). The stoichiometry of the metal ion to ligand was 1:1. The solution was heated to reflux for three hours. A red precipitate was formed on cold and washed with small portions of methanol then ether. The yield was 1.42 g (69%) and the melting point was over 320 °C.

2.3.2. Reaction of oxovandium(IV) with H₃L ligand

Oxovandium(IV) sulphate monohydrate, VOSO₄.H₂O, (0.489 g, 3 mmol) in a least amount of distilled water, just to dissolve VOSO₄.H₂O, was added gradually with constant stirring to a solution of the deprotonated H₃L ligand (0.894 g, 3 mmol) in methanol (60 mL). The solution was heated to reflux

for three hours. A green precipitate was obtained and washed with small portions of methanol then ether. The yield was 1.56 g (69.03%) and the melting point was over 320 °C.

2.4. Physical measurements

The analyses of carbon, hydrogen, nitrogen and sulfur were carried out at the National Research Center, Giza, Egypt. Analyses of metal ions were performed after the dissolution of the solid complex in hot concentrated nitric acid, HNO₃. The metal ions were then titrated with EDTA [24-26]. The FT-IR spectra (4000-400 cm⁻¹) of the compounds were recorded as KBr discs using FT-IR (Shimadzu) spectrophotometer model 4000. Absorption frequencies are given in wavenumbers (cm⁻¹). ¹H NMR spectra were recorded using a Varian spectrometer, 200 MHz. DMSO-d_6 was used as a solvent and tetramethylsilane (TMS) as an internal reference. The spectra were extended from 0-15 ppm. The chemical shifts (δ) are given down field relative to TMS. D₂O was added to every sample to test for the deuteration of the samples. The electronic spectra of the ligand and their metal complexes were carried out on a JASCO model V-550 UV-VIS spectrophotometer in the range 200-900 nm. Magnetic susceptibilities of the complexes were measured by the Gouy method at room temperature using Johnson Matthey, Alfa product, Model No. (MKI), Magnetic Susceptibility Balance. The diamagnetic corrections were calculated from Pascal's constants for all atoms in the compounds [27]. Conductivities were measured in solutions of the compounds in DMF (1×10^{-3} M) using WTWD-812 Weilheium-conductivity meter model LBR, fitted with a cell model LTA100. Thermal gravimetric analysis (TGA) data was measured from room temperature up to 800 °C at a heating rate of 20 °C/min. The data were obtained using a Shimadzu TGA-50H instrument. All melting points were recorded in open capillary tubes on a Stuart SMP3 melting point apparatus. ESR spectra of compounds were recorded on the Bruker, Model: EMX, X-band spectrometer. Mass spectra of the compounds were recorded on a Hewlett Packard mass spectrometer model MS 5988. Samples were introduced directly to the probe, and the fragmentations were carried out at 300 °C and 70 eV.
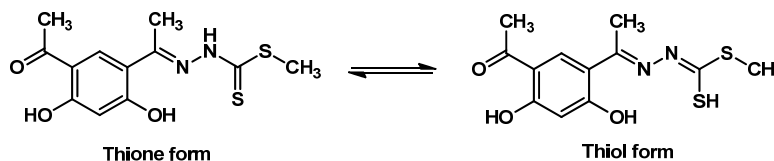
2.5. Biological activity

The standardized disc-agar diffusion method [28] was followed to investigate the activity of the current compounds against the sensitive organisms *Staphylococcus aureus* (ATCC 25923) and *Streptococcus pyogenes* (ATCC 19615) as Gram-positive bacteria, *Pseudomonas phaseolicola* (GSPB 2828) and *Pseudomonas fluorescens* (S 97) as Gram-negative bacteria and the fungi *Fusarium oxysporum* and *Aspergillus fumigatus*. The antibiotic cephalothin was used as standard reference control in the case of Gram-positive bacteria and chloramphencol was used as standard reference control in the case of Gram-negative bacteria, cycloheximide was used as standard antifungal reference control.

The tested compounds were dissolved in DMF to get concentrations of 1 and 2 mg/mL.

Table 1. Physical and analytical data of the hydrazone, H_3L, ligand and its transition metal complexes.

Ligand/Complex	Molecular formula	M.wt. (Yield %)	Color	M.p. (°C)	Elemental Analyses, Found (Calcd.) %				
					C	H	N	S	M
H_3L	$C_{12}H_{14}N_2O_3S_2$	298.37 (59)	Yellow	226-227	47.83 (48.30)	4.70 (4.72)	9.36 (9.39)	22.01 (21.49)	-
$[Cu(HL)]_2$	$C_{24}H_{24}N_4O_6S_4Cu_2$	719.72 (65)	Dark Green	>320	39.61 (40.00)	3.56 (3.35)	7.60 (7.89)	18.20 (17.82)	17.52 (17.64)
$[Ni(HL)]_2.2H_2O$	$C_{24}H_{28}N_4O_8S_4Ni_2$	746.16 (63)	Red	>320	37.83 (38.63)	3.52 (3.78)	7.59 (7.50)	17.04 (17.18)	15.69 (15.73)
$[Co(H_2L)(H_2O)_2]_2(NO_3)_2.2H_2O$	$C_{24}H_{38}N_6O_{18}S_4Co_2$	946.72 (70)	Green	>320	30.20 (30.44)	3.92 (4.04)	8.65 (8.87)	13.20 (13.54)	12.80 (12.65)
$[VO(HL)]_2$	$C_{24}H_{24}N_4O_8S_4V_2$	726.50 (69)	Green	>320	39.70 (39.67)	3.65 (3.30)	7.76 (7.70)	18.00 (17.61)	NA* (14.01)
$[Fe(H_2L)(CH_3OH)NO_3]_2.2H_2O.CH_3OH$	$C_{27}H_{40}N_6O_{17}S_4Fe_2$	960.87 (57)	Red	>320	34.28 (33.74)	3.96 (4.19)	8.25 (8.74)	12.41 (13.34)	11.30 (11.65)
$[Zn(HL)]_2.6H_2O$	$C_{24}H_{36}N_4O_{12}S_4Zn_2$	830.81 (69)	Yellow	>320	34.05 (34.69)	4.82 (4.36)	6.24 (6.74)	14.32 (15.43)	15.16 (15.64)
$[Cd(HL)]_2.H_2O$	$C_{24}H_{26}N_4O_7S_4Cd_2$	834.74 (76)	Yellow	>320	35.01 (34.50)	3.30 (3.11)	5.97 (6.71)	15.03 (15.36)	26.52 (26.83)

Scheme 2

The test was performed on medium potato dextrose agar (PDA) which contains infusion of 200 g potatoes, 6.00 g dextrose and 15.0 g agar [29]. Uniform size filter paper disks (3 disks per compound) were impregnated by equal volume (10 μL) from the specific concentration of dissolved tested compounds and carefully placed on incubated agar surface.

After incubation for 36 h at 27 °C in the case of bacteria and for 48 h at 24 °C in the case of fungi, inhibition of the organisms which evidenced by clear zone surround each disk was measured and used to calculate mean of inhibition zones [28,29]. The activity of tested compounds was categorized as follows: (i) Low activity = Mean of zone diameter ≤ 1/3 of mean zone diameter of control. (ii) Intermediate activity = Mean of zone diameter ≤ 2/3 of mean zone diameter of control. (iii) High activity = Mean of zone diameter > 2/3 of mean zone diameter of control.

3. Results and discussion

3.1. The hydrazone H_3L ligand

The hydrazone, H_3L, ligand was synthesized by the condensation of *S*-methyldithiocarbazate with 4,6-diacetyl resorcinol in the molar ratio 2:1 or 1:1. In both cases, the obtained product was found to be 1:1 as investigated from elemental analysis and spectral data. The structure of the hydrazone, H_3L, ligand was identified by elemental analyses, infrared, UV-Visible, ^1H NMR and mass spectra. Table 1 lists the physical and analytical data of the H_3L ligand and its transition metal complexes. It is expected that the H_3L ligand has two tautomers, thione and thiol, forms. The thione is the dominant form in either solid state or solution, while the thiol form became more dominant and mainly the most effective in presence of metal ions [30-32]. The H_3L ligand is dibasic tridentate with ONS sites. Scheme 2 is representative structures of the thione-thiol forms of the H_3L ligand.

The infrared frequencies of the present H_3L ligand along with *S*-methyldithiocarbazate (SMDTC), 4,6-diacetylresorcinol (DAR) and their tentative assignments are listed in Table 2. The infrared spectra are consistent with the formation of H_3L ligand. The vibrational assignments were aided by comparison with the vibrational frequencies of the related compounds, such as, the hydrazones of *S*-methyldithiocarbazate and

hydrazones of 4,6-diacetylresorcinol [11,33-36]. The fundamental stretching mode of the azomethine moiety, $\nu(C=N)$, is readily assigned by comparison with the infrared spectra of *S*-methyldithiocarbazate and 4,6-diacetylresorcinol. This intense band at 1602 cm^{-1} for H_3L ligand was assigned to the C=N stretching frequency of the ligand and are characterized for the azomethine moiety of most hydrazone compounds. The absorption band of the C=O appeared at 1643 cm^{-1} in the infrared spectrum of the ligand, which gave an indication that one of the C=O groups in the 4,6-diacetylresorcinol was involved in the condensation reaction while the other one still free, and its stretching frequency still persist with slightly lower frequency than the free 4,6-diacetylresorcinol, Δν = 24 cm^{-1}. The $\nu(NH_2)$ stretching frequencies of *S*-methyldithio carbazate which lies at 3307 and 3241 cm^{-1} were also disappeared after the formation of the H_3L ligand. One band was observed at 3319 cm^{-1} which is assigned to $\nu(NH)$ in the infrared spectrum of the ligand. On the other hand, other fundamental bands were assigned in the infrared spectra of H_3L ligand which are listed in Table 2.

The mass spectrum of the hydrazone, H_3L, ligand, revealed the molecular ion peaks at m/e 298, which is coincident with the formula weight (298.37) for H_3L ligand and supports the identity of the structure. The fragmentation pattern of the mass spectrum of the H_3L ligand is depicted in Scheme 3.

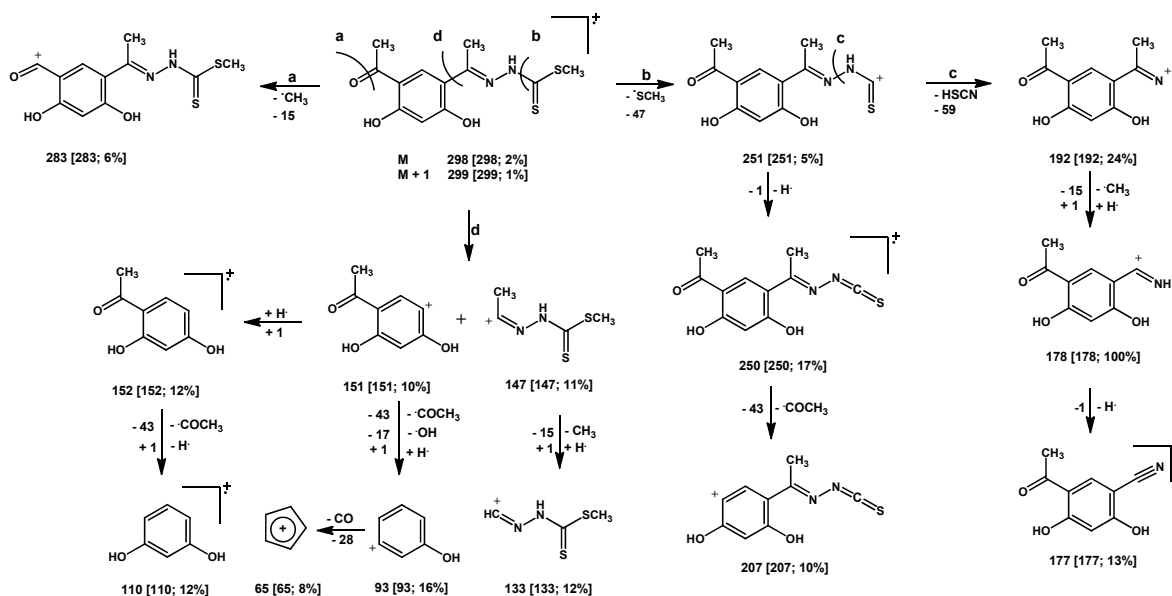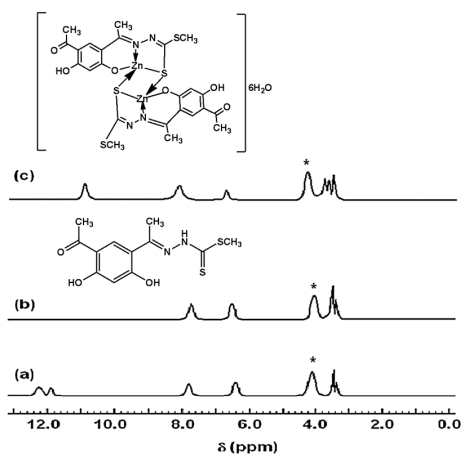^1H NMR spectra of H_3L ligand in deuterated dimethyl sulphoxide, DMSO-d_6, without and with D_2O are shown in Figure 1. The chemical shifts of the proton signals in the spectrum of the hydrazone, H_3L, ligand with their assignments are listed in Table 3. Both signals of the -OH for the phenolic protons which lies at 12.56 ppm and signal of the -NH proton which lies at 12.36 ppm in the ligand were disappeared in the presence of D_2O. ^1H NMR spectra do not show any resonance near to ~4.0 ppm attributable to the S-H proton resonance, indicating that the thione form still persists in solution.

Electronic spectral data of the H_3L ligand was recorded in DMF solution. Two absorption bands were observed at 299 and 355 nm. The first band corresponds to the π → π* transition of the C=N, C=S and C=O groups, and the second band corresponds to the n → π* transitions resulting from nitrogen, oxygen and sulfur atoms, which are overlapped with the intermolecular charge transfer (CT) from the phenyl ring [37-39].

Table 2. Infrared frequencies (cm⁻¹) of H₃L ligand, S-methyldithiocarbazate (SMDTC) and 4,6-Diacetylresorcinol (DAR), and their tentative assignments *.

H₃L	SMDTC	DAR	Assignments
3423 w, br	-	3222 w, br	ν(OH)
-	3307 m, 3241 m	-	ν(NH₂)
3319 s	3179 m, br	-	ν(NH)
3043 w	-	3083 w	ν(ArC-H)
2921 m	2914 w	-	-
1643 s	-	1667 vs	ν(C=O)
1602 w	-	-	ν(-C=N-)
1469 m, 1421 w	1469 s	1490 m	δ(CH₃) asym. and δ (CH₂) asym.
1338 m	1340 m	-	ν(C=S)
1262 w	-	1258 vs	δ(OH) in plane
1185 w	1170 w	1180 m	ν(C-N) and ν (C-C)
1068 s	1046 s	-	ν(N-N)
1028 w	-	1030 w, sh	δ(ArC-H) in plane
952 m, 890 w	966 w, 910 w	951 w, 903 w	ρr(CH₃) and ρr(CH₂)
510 w	-	423 w	δ(OH) out of plane

* s = strong, m = medium, w = weak, vs = very strong, sh = shoulder, br = broad.

Scheme 3

Figure 1. ¹H NMR spectra (δ, ppm) in DMSO-d_6 solvent of: (a) H₃L ligand without addition of D₂O, (b) H₃L ligand after the addition of D₂O and (c) [Zn(HL)]₂.6H₂O complex (**6**); (*) Suppressed H₂O.

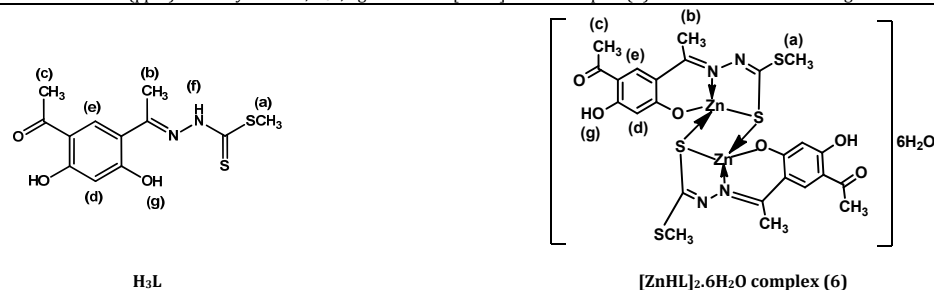### 3.2. Metal complexes of H₃L ligand

The hydrazone, H₃L, ligand behaves as a dibasic with tridentate ONS sites. The ligand reacts with Cu(II), Ni(II),

Co(II), Zn(II), Cd(II), Fe(III) and VO(IV) ions to yield the corresponding transition metal complexes. The isolated transition metal complexes were identified by elemental analyses, FT-IR, ¹H NMR, mass, UV-Visible, ESR spectroscopy and thermal gravimetric analysis (TGA), beside, the magnetic susceptibility and molar conductivity measurements. The physical and analytical data of the transition metal complexes are listed in Table 1.

3.2.1. Infrared spectra

The characteristic vibrational frequencies and their assignments for the synthesized transition metal complexes are listed in Table 4. The assignments were aided by comparison with the vibrational frequencies of the free ligand and other related compounds such as transition metal complexes of 4,6-diacetylresorcinol hydrazones and 6-methyl-4-formylpyrimidine of *S*-methyldithiocarbazate [33,40]. Inspection of the data reveals that, the stretching frequencies of azomethine group of the metal complexes, ν(-C=N-), are shifted to lower frequencies at the range 1563-1535 cm⁻¹ and are in lower frequencies, than the corresponding ν(-C=N-) frequency of the H₃L ligand which lie at 1602 cm⁻¹. This lowering shift may be due to the coordination of the azomethine group to the metal ion [41-43].

Table 3. The ^{1}H NMR chemical shifts (ppm) of the hydrazone, H_3L, ligand and its $[ZnHL]_2.6H_2O$ complex (**6**) in DMSO-d_6 and their assignments *.

H_3L $[ZnHL]_2.6H_2O$ complex (**6**)

Chemical shifts (ppm)		Assignments
H_3L	$[ZnHL]_2.6H_2O$ (**6**)	
2.52	2.48	(s, 3H, SCH$_3$) (a) H$_3$L, (s, 6H, 2 SCH$_3$) (a) (**6**)
2.61	2.59	(s, 3H, CH$_3$) (b) H$_3$L, (s, 6H, 2 CH$_3$) (b) (**6**)
2.64	2.69	(s, 3H, CH$_3$) (c) H$_3$L, (s, 6H, 2 CH$_3$) (c) (**6**)
6.39	6.04	(s, 1H, 1 Ar-H) (d) H$_3$L, (s, 2H, 2 Ar-H) (d) (**6**)
8.13	8.12	(s, 1H, 1 Ar-H) (e) H$_3$L, (s, 2H, 2 Ar-H) (e) (**6**)
12.36	-	(s, 1H, NH) exchangeable by D$_2$O (f) H$_3$L
12.56	12.67	(s, 1H, OH) exchangeable by D$_2$O (g) H$_3$L, (s, 2H, 2 OH) exchangeable by D$_2$O (g) (**6**)

* s = singlet, Data given for the spectrum depicted in Figure 1. Chemical shifts (ppm) were referenced at 25 °C with respect to TMS.

Table 4. Characteristic infrared frequencies (cm^{-1}) ^{a} of the hydrazone, H_3L, ligand and its transition metal complexes.

Ligand/ Complex	ν(OH)	ν(C=O)	ν(C=N)	ν(CH) aliph.	ν(CH) Ar.	ν(C-S)	ν(C-S-C)	ν(N-N)	ν(M-N)	ν(M-O)	Other significant bands
H_3L ^{b}	3423 w, br	1643 s	1602 s	2921m, 2851 w	3043 w	-	952 m	1068 m	-	-	-
$[Cu(HL)]_2$	3447 w, br	1640 s	1540 s	2920 w	3093 w	676 w	993 m	1085 w	604 m	485 w	-
$[Ni(HL)]_2.2H_2O$	3440 w, br	1638 s	1535 s	2920 m	-	687 w	958 w	1084 w	607 m	467 w	-
$[Co(H_2L)(H_2O)_2]_2(NO_3)_2.2H_2O$	3423 s, br	1629 m	1539 s	2927 w	-	670 w	964 w	1085 w	602 w	470 w	NO$_3^-$ (ionic) 1754 (s), 1384 (s), 836 (s)
$[VO(HL)]_2$	3404 w, br	1642 s	1538 s	2918 w	3091 w	677 w	957 w	1083 w	604 w	485 w	993 (s) for ν(V=O)
$[Fe(H_2L)(CH_3OH)NO_3]_2.2H_2O.CH_3OH$	3386 s, br	1642 s	1563 s	2927 w	-	665 w	962 m	1085 w	576 w	491 w	NO$_3^-$ (unidentate) 1426, 1320, 809
$[Zn(HL)]_2.6H_2O$	3422 s, br	1633 s	1554 s	2927 w	-	679 w	964 m	1085 w	590 m	488 w	-
$[Cd(HL)]_2.H_2O$	3420 s, br	1618 s	1548 s	2926 w	-	670 w	966 m	1084 w	580 m	470 w	-

^{a} s = strong, m = medium, w = weak, br = broad.
^{b} Stretching frequencies of the ν(NH) and ν(C=S) of the H$_3$L ligand which observed at 3319 and 1338 cm^{-1}; respectively, were disappeared in all the infrared spectra of the metal complexes.

The broad bands in the range of 3447-3386 cm^{-1} can be assigned to the stretching frequencies of the ν(OH) of water and/or methanol molecules associated to the complexes which are also confirmed by the elemental analyses. The ν(C=S) band at 1338 cm^{-1} for H$_3$L ligand was not observed in the metal complexes, thus supporting the suggestion of coordination through the thiol sulfur and showed the ν(C-S) band in the range of 687-665 cm^{-1}. The shift frequency of ν(N-N) band in all the metal complexes to higher frequency in the range 1085-1083 cm^{-1} compared to the ν(N-N) band in the free ligand at 1068 cm^{-1}, is another evidence to that the coordination involves thiol sulfur and not the thione sulfur. The weak bands in the ranges 491-467 cm^{-1} and 607-576 cm^{-1} were assigned to the ν(M-O) and ν(M-N) stretching frequencies of the metal-oxygen and metal-nitrogen bonds for the transition metal complexes of the H$_3$L ligand [44]. This emphasized supporting that the bonding sites of the ligand to the metal ions is achieved by the phenolic oxygen atom, the azomethine nitrogen atom and thiol sulfur atom of the ligand.

The free NO$_3^-$ exhibited three bands at 1754, 1381 and 836 cm^{-1} in [Co(H$_2$L)(H$_2$O)$_2$]$_2$(NO$_3$)$_2$2H$_2$O complex (**3**), and the unidentate NO$_3^-$ ions exhibited three bands at 1426, 1320 and 809 cm^{-1} in [Fe(HL)(CH$_3$OH)(NO$_3$)]$_2$.H$_2$O.CH$_3$OH complex (**5**) [44,45].

The IR spectrum of VO(IV) complex (**4**) displayed a band at 993 cm^{-1} which have no counterpart in the spectrum of the H$_3$L ligand and is assigned to the stretching frequency of the ν(V=O) band [44].

3.2.2. Electronic, ESR, mass spectra and magnetic moment measurements and molar conductance

Table 5 lists the electronic spectral bands of the metal complexes in Nujol mulls and in DMF solution and the magnetic moments of the metal ions in their complexes. The absorption spectra exhibit no obvious difference on going from Nujol mulls to DMF solution.

The electronic spectrum of the dimer dark green [Cu(HL)]$_2$ complex (**1**) showed one band due to E$_g$ → ^{3}T$_{2g}$(G) transition, which was observed at 598 nm which confirms square planar structure [46,47]. The subnormal magnetic moment of Cu(II) complex representing in a strong metal-metal interaction. Elemental analysis and spectral data confirm square planar structure for the Cu(II) complex [46-48]. X-Band ESR spectra of [Cu(HL)]$_2$ (**1**) complexes are silent due to strong metal-metal bond in dimeric form.

The electronic spectrum of the red [Ni(HL)]$_2$.2H$_2$O complex (**2**), is consistent with the square planar transitions. One electronic transition band was observed at 499 nm, which was assigned to ^{1}A$_{1g}$ → ^{1}A$_{2g}$ transition [49]. In most cases, it is rarely possible to identify the d-d transitions of nickel(II) square planar complexes in presence of organic ligands, since even the very weak tail of UV-organic absorption tailing into the visible can obscure them.

Table 5. Electronic (d-d) transition bands (nm) [a] and magnetic moments (B.M.) of the transition metal complexes of the hydrazone, H_3L, ligand.

Complex	λ_{max} (nm) Nujol mulls (DMF nm; ε_{max})	Assignments	Magnetic moments (B.M.)		Conductance ohm^{-1}·cm^2·mol^{-1}	Geometry
			$\mu_{compl.}$ [b]	$\mu_{eff.}$ [c]		
$[Cu(HL)]_2$	598 (589; 0.0058)	$E_g \rightarrow {}^3T_{2g}(G)$ [d]	Diamag.	Diamag.	1.35	Square planar
$[Ni(HL)]_2.2H_2O$	499 (423; 0.0036)	${}^1A_{1g} \rightarrow {}^1A_{2g}$	Diamag.	Diamag.	2.65	Square planar
$[Co(H_2L)(H_2O)_2]_2(NO_3)_2 2H_2O$	454 (420; 0.0070), 608 (600; 0.0043)	${}^4T_{1g}(F) \rightarrow {}^4T_{1g}(P)$ [e] ${}^4T_{1g}(F) \rightarrow {}^4A_{2g}(F)$	5.98	4.70	141.00	Octahedral
$[VO(HL)]_2$	591 (595; 0.0048)	$b_2 \rightarrow b_1$	Diamag.	Diamag.	1.65	Square pyramid
$[Fe(H_2L)(CH_3OH)NO_3]_2.2H_2O.CH_3OH$	518 (501; 0.0067), 553 (523; 0.0088)	Charge transfer (CT) band tailing from UV to visible region.	3.73	2.64	14.00	Octahedral
$[Zn(HL)]_2.6H_2O$	-	-	Diamag.	Diamag.	2.65	Tetrahedral
$[Cd(HL)]_2.H_2O$	-	-	Diamag.	Diamag.	4.52	Tetrahedral

[a] Electronic (*d-d*) transition bands of the complexes are in (nm) and were recorded in the solid state as Nujol mulls and DMF value in parentheses are the wave number in DMF solvent and ε_{max} values were multiplied by 10^{-4} (mol^{-1}·cm^{-1}). The electronic absorption bands due to the hydrazone ligand in the complexes were observed in each spectrum in the UV region and were not cited in the table.

[b] $\mu_{compl.}$ is the magnetic moment of all metal ions present in the complex.

[c] $\mu_{eff.}$ is the magnetic moment of one metal ion in the complex.

[d] Racha parameter (Dq) of Cu(II) (1) complex is 589 nm.

[e] Racha parameters for Co(II) complex (3) β, B, Dq and ν_1 are 1.02, 1144, 915 and 1266; respectively.

The red nickel(II) complex (**2**) is diamagnetic suggesting a square planar geometry around the nickel(II) ion.

The electronic spectrum of the green Co(II) complex (**3**) showed that, the complex has two bands at 454 and 608 nm indicating an octahedral geometry. The transitions can be interpreted by using Tanab-Sugano diagram. In the Co(II) octahedral complexes, the spectra usually consist of three bands [50]. The third band, which is due to ${}^4T_{1g}(F) \rightarrow {}^4T_{2g}(F)$ transition, was not observed due to the fact that it occurs in the near infrared region, and out of the range of the used instrument. The other two bands were observed in the visible region, The former band due to ${}^4T_{1g}(F) \rightarrow {}^4T_{1g}(P)$ transition was observed at 454 nm and is slightly obscured by UV-organic ligand transitions. The second one due to ${}^4T_{1g}(F) \rightarrow {}^4A_{2g}(F)$ transition, was observed at 608 nm for complex (**3**). Rach parameters for complexes (**3**) were calculated which gave the values 1.02, 1144, 915, 1266 for β, B, Dq, ν_1; respectively. The Co(II) complex showed the magnetic moment 4.7 B.M., emphasizing that the complex is octahedral [51].

The electronic spectrum of the green oxovanadium(IV) complex (**4**) showed one band at 591 nm; which corresponds to $b_2 \rightarrow b_1$ electronic transition [52]. With the aid of the elemental analysis and the infrared spectra, the oxovanadium(IV) complex (**4**) is 5-coordinate which would be square pyramid [53]. Oxovanadium(IV) complex is diamagnetic due to strong V-V bond in dimeric form. X-Band ESR spectra of $[VO(HL)]_2$ (**4**) complexes are silent due to strong metal-metal bond in the dimeric form.

The electronic spectrum of the red Fe(III) complex (**5**) showed two medium bands at 518 and 553 nm. It was not possible to identify the type of the d-d transition, due to a strong charge transfer (CT) band tailing from the UV-region to the visible region [51]. Generally, from the elemental and infrared spectrum which gave significant proof for the nitrate anion to act as a unidentate ligand, it is expected that the Fe(III) complex (**5**) has octahedral arrangement. Magnetic moment of the Fe(III) complex was measured and gives 5.34 B.M. This value refer to that the Fe(III) complex (**5**) is high spin octahedral geometry [51].

The yellow $[Zn(HL)]_2.6H_2O$ (**6**) and $[Cd(HL)]_2.H_2O$ (**7**) complexes, are diamagnetic as expected and their geometries are most probably tetrahedral for Zn(II) complex (**6**) and Cd(II) complex (**7**). ^1H NMR spectrum of $[Zn(HL)]_2.6H_2O$ (**6**) in DMSO-d_6 is depicted in Figure 1. The chemical shifts of the proton signals in the spectrum and their assignments are listed in Table 3. It is worthnoting that the signal of one phenolic proton was observed in the spectrum while the other phenolic and amino (thiol tautomer) protons were not observed in the ^1H NMR spectrum of the Zn(II) complex, which means that these protons were deprotonated to coordinate with the Zn(II) ion.

The molar conductance of the complexes was measured in DMF, 1×10^{-3} M, which gave low values (12.52-1.35) ohm^{-1}cm^{2}mol^{-1}. However, the molar conductance value Co(II) complex (**3**) are 141 ohm^{-1}cm^{2}mol^{-1} which fall within the range of 1:1 electrolytes which indicate that NO_3^- ion is completely in the outer sphere [54].

3.2.3. Thermal gravimetric analysis

Figure 2 depicts the TGA-DrTGA curves of (A) $[Fe(HL)(CH_3OH)(NO_3)]_2.H_2O.CH_3OH$ complex (**5**) and (B) $[Cd(HL)]_2.H_2O$ complex (**7**). Thermal gravimetric analysis (TGA) for $[Ni(HL)]_2.2H_2O$ complex (**2**), shows four stages. The first stage is due to the loss of two uncoordinated water molecules (weight loss; Calcd./Found%; 4.82/4.83%) which observed at 27-100 °C. The second stage was observed at 212-324 °C and is due to the loss of $(CH_3S)_2$ molecule. (weight loss; Calcd./Found%; 12.59/ 12.35%). The third stage was observed at 324-523 °C and is due to loss of one $(CN)_2$ molecule of two CH_3CN molecules and CH_3CHO from the complex molecules (weight loss; Calcd./Found%; 29.48/28.76%). The fourth stage was observed at 523-800 °C and is due to loss $C_6H_8O_2$ molecules (weight loss; Calcd./Found%; 14.74/14.42%). The residue due to the decomposition of the rest part of the complex was $[NiOSC_2]_2$ (weight loss; Calcd./Found%; 38.24/38.90%).

TGA of $[Co(H_2L)(H_2O)_2]_2(NO_3)_2.2H_2O$ complex (**3**), shows three stages. The first stage is due to the loss of two uncoordinated water molecule (weight loss; Calcd./Found%; 3.80/3.88%) which observed at 26-120 °C. The second stage was observed at 175-329 °C and is due to the loss of four coordinated water molecules and two CH_3SCN molecules (weight loss; Calcd./Found%; 23.02/23.49%). The third stage was observed at 330-800 °C and is due to loss of two CH_3CN, N_2O_5, CH_3CO and C_6H_3OH molecules (weight loss; Calcd./Found%; 40.56/41.13%). The residue due to the decomposition of the rest part of the complex showed some organic fragment associated with the metal oxide and metal sulfide (weight loss; Calcd./Found%; 32.30/32.75%).

TGA of $[Fe(HL)(CH_3OH)(NO_3)]_2.H_2O.CH_3OH$ complex (**5**), shows three stages. Figure 2A depicts the TGA-DrTGA curves of $[Fe(HL_c)(CH_3OH)(NO_3)]_2.H_2O.CH_3OH$ complex (**5**). The first stage is due to the loss of one uncoordinated methanol molecule and one uncoordinated water molecule (weight loss; Calcd./Found%; 5.31/5.00%) which observed at 52-100 °C. The second stage was observed at 182-255 °C and is due to the loss of two coordinated methanol molecules and one $(CH_3S)_2$ molecule (weight loss; Calcd./Found%; 16.79/17.50%).

Table 6. Temperatures of decomposition and the kinetic parameters of complexes **2**, **3**, **5** and **7**.

Compound	Step	T (K)	A (1/s)	ΔE (kJ/mol)	ΔH (kJ/mol)	ΔS (kJ/mol.K)	ΔG (kJ/mol)
[Ni(HL)]₂.2H₂O	First	350	3.122	16.88	13.96	-245	99.71
	Second	576	1.8×10⁵	76.90	72.11	-158	163.29
	Third	674	2291	65.91	60.30	-196	192.42
	Fourth	937	9.577	53.61	45.81	-244	274.43
[Co(H₂L)(H₂O)₂]₂(NO₃)₂.2H₂O	First	364	1.8	19.11	16.08	-250	107.08
	Second	562	1177	27.83	23.15	-200	140.23
	Third	811	30.96	65.35	58.60	-233	247.86
[Fe(H₂L)(CH₃OH)NO₃]₂.2H₂O.CH₃OH	First	441	0.07	10.91	7.24	-270	126.31
	Second	516	23.82	33.13	28.83	-230	148.42
	Third	655	3.90	20.37	14.92	-248	177.36
[Cd(HL)]₂.H₂O	First	325	0.367	20.15	17.44	-260	101.94
	Second	595	14.10	33.58	28.63	-245	174.41
	Third	668	112	51.84	46.28	-220	193.24

The third stage was observed at 255-800 °C and is due to the dissociation of the organic ligand within the complex (weight loss; Calcd./Found%; 61.66/61.72%). The residue was iron oxide (weight loss; Calcd./Found%; 17.01/17.07%).
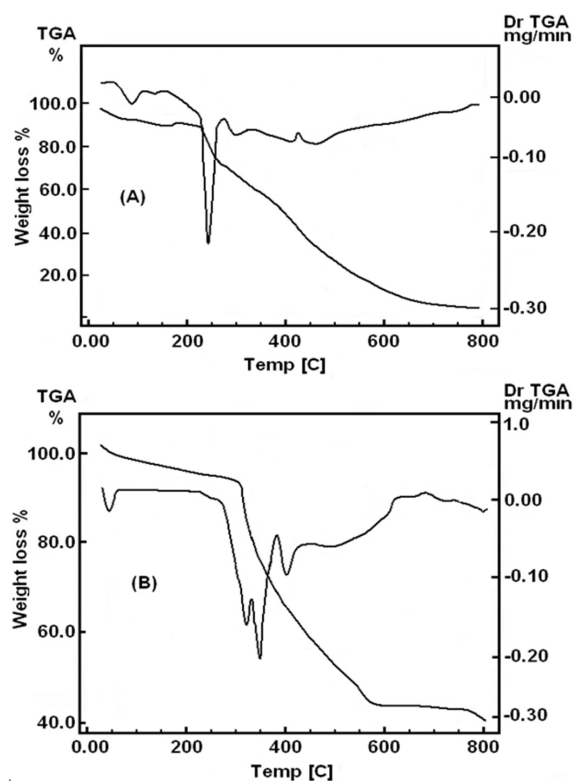

Figure 2. TGA-DrTGA of curves (A) [Fe(H₂L)(CH₃OH)NO₃]₂.H₂O.CH₃OH complex (**5**) and (B) [Cd(HL)]₂.H₂O complex (**7**).

TGA of [Cd(HL)]₂.H₂O complex (**7**), shows three stages. Figure 2B depicts the TGA-DrTGA curves of [Cd(HL)]₂.H₂O complex (**7**). The first stage is due to the loss of one uncoordinated water molecule (weight loss; Calcd./Found %; 2.15/1.76%) which observed at 50-80 °C. The second stage was observed at 247-354 °C and is due to the loss of two CH₃SCN molecules and two CH₃CN molecules (weight loss; Calcd./Found%; 27.31/26.08%). The third stage was observed at 354-600 °C and is due to loss of two CH₃CHO molecules, SO₂ and C₆H₄ molecules from the complex molecules (weight loss; Calcd./Found%; 27.31/27.63%). The residue was observed due to the decomposition of the rest part of the complex (weight loss; Calcd./ Found%; 43.60/44.00%).

In order to access the influence of the type of the metal on the thermal behavior of the complexes, the order *n*, and the activation parameters of the various decomposition stages were determined from the TG thermograms using the Coats-Redfern equations in the following forms:

$$\ln[1-(1-\alpha)^{1-n}/(1-n)T^2] = M/T + B \qquad \text{for } n \neq 1 \qquad (1)$$

$$\ln[-\ln(1-\alpha)/T^2] = M/T + B \qquad \text{for } n = 1 \qquad (2)$$

where M = -E/R and B = ln AR/Φ E; E, R, A and Φ are the heat of activation, the universal gas constant, pre-exponential factor and heating rate, respectively [55,56].

The correlation coefficient, *r*, was computed using the least square method for different values of *n* by plotting the left–hand side of Equation (1) or (2) versus 1000/T, Figure 3. The *n* values, which gave the best fit ($r \approx 1$). From the intercept and linear slope of such stage, the A and E values were determined. The other kinetic parameters, ΔH, ΔS and ΔG were computed using the relationships; ΔH = *E* – RT, ΔS = R[ln(Ah/kT)-1] and ΔG = ΔH - TΔS, where k is the Boltzmann's constant and h is the Plank's constant. The kinetic parameters are listed in Table 6. The following remarks can be pointed out: (1) All complexes decomposition stages show a best fit for (n = 1) indicating a first order decomposition in all cases. (2) The value of ΔH increases significantly for the subsequently decomposition stages. (3) The negative values of activation entropies ΔS indicate a more order activated complex than reactants and/or the reaction are slow. (4) The positive values of ΔH means that the decomposition processes are endothermic [55,56].

Finally, on the basis of elemental analysis and infrared, mass, electronic spectra, ESR for copper(II) and oxovanadium(IV) complexes and TGA for complex **2**, **3**, **5** and **7**, it is possible to draw up the tentative structures of the transition metal complexes. Figure 4 depicts the proposed structures of the metal complexes.

3.3. Biological activity

The hydrazone, H₃L, ligand and its metal complexes were evaluated for sensitive organisms, which are: two strain Gram-positive bacteria (*Staphylococcus aureus* and *Streptococcus pyogenes*), Gram-negative bacteria (*Pseudomonas phaseolicola* and *Pseudomonas fluorescens*) and two fungi (*Fusarium oxysporum* and *Aspergillus fumigatus*). The activity of the hydrazone, H₃L, ligand and its metal complexes against the used organisms as depicted in Table 7. The hydrazone, H₃L, ligand was found to be biologically active and some metal complexes exhibit mild antimicrobial activity. Although Ni(II) (**2**), Co(II) (**3**) complexes showed high antimicrobial activities, the Fe(III) complex (**5**) showed a dramatic low activity for all Gram-positive, Gram-negative bacteria and fungus strain. Cd(II) complex (**7**) showed high activity in Gram-positive bacteria in high and low concentrations and low activity for Gram-negative and fungi. Most of the complexes showed low activity towards the fungi.
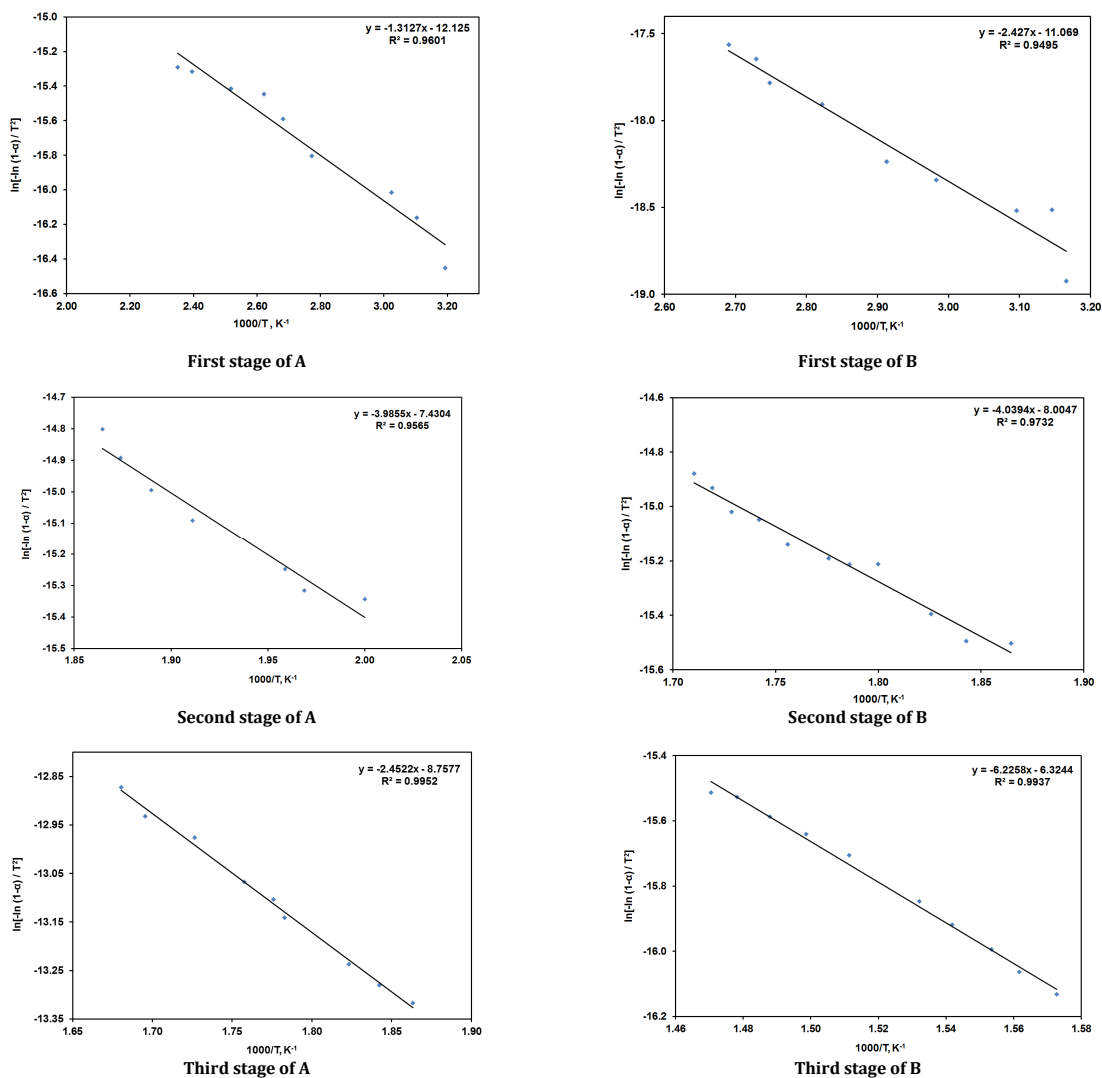
Figure 3. Costs-Redfern plots for (A) [Fe(H$_2$L)(CH$_3$OH)NO$_3$]$_2$.H$_2$O.CH$_3$OH (**5**) and (B) [Cd(HL)]$_2$.H$_2$O (**7**).
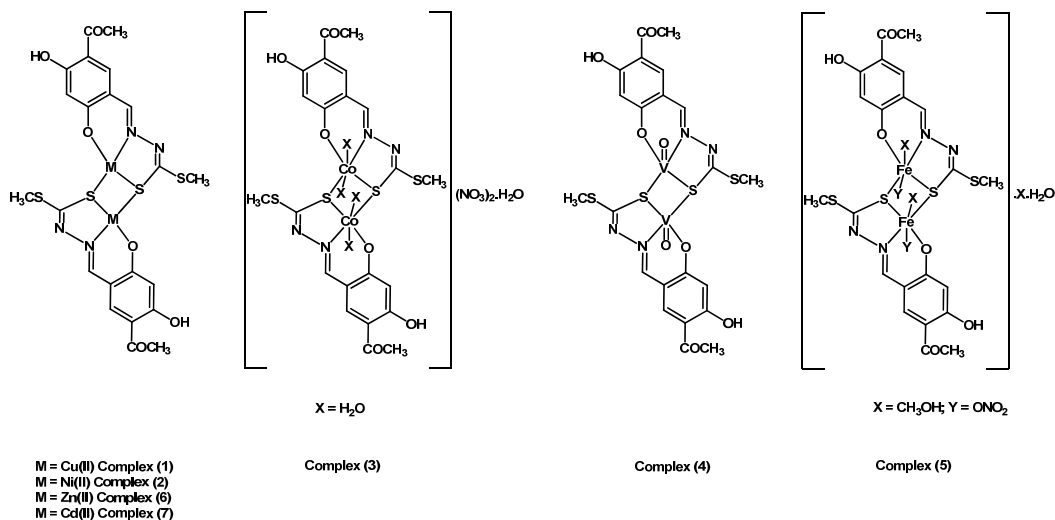

Figure 4. Structures of the metal complexes of H$_3$L ligand.

Table 7. Biological activity of the synthesized hydrazone complexes **1-7** [a].

Organisms	Mean of zone diameter, nearest whole mm											
	Gram-positive bacteria				Gram-negative bacteria				Fungi			
	Staphylococcus aureus (ATCC 25923)		*Streptococcus pyogenes* (ATCC 19615)		*Pseudomonas Phaseolicola* (GSPB 2828)		*Pseudomonas fluorescens* (S 97)		*Fusarium oxysporum*		*Aspergillus fumigatus*	
	A	B	A	B	A	B	A	B	A	B	A	B
H_3L	18-I	14-I	29-H	22-H	15-I	15-I	24-I	18-I	22-I	12-I	17-I	13-I
$[Cu(HL)]_2$	25-I	16-I	24-I	18-I	18-I	13-I	27-H	16-I	12-L	13-I	15-I	9-L
$[Ni(HL)]_2.2H_2O$	30-H	23-H	26-H	28-H	32-H	18-H	28-H	23-H	14-I	17-I	17-I	12-I
$[Co(H_2L)(H_2O)_2]_2(NO_3)_2.2H_2O$	25-I	23-H	27-H	26-H	17-I	22-H	28-H	17-I	20-I	14-I	12-L	8-L
$[VO(HL)]_2$	22-I	14-I	15-I	14-I	16-I	10I	13-I	12-I	15-I	12-I	8-L	5-L
$[Fe(H_2L)(CH_3OH)NO_3]_2.2H_2O.CH_3OH$	19-I	16-I	13-I	3-L	4-L	9-L	6-L	8-L	8-L	6-L	2-L	3-L
$[Zn(HL)]_2.6H_2O$	21-I	15-I	9-L	14-I	12-I	14-I	19-I	15-I	20-I	10-I	10-I	9-L
$[Cd(HL)]_2.H_2O$	28-H	22-H	28-H	24-H	15-I	22-I	22-I	14-I	16-I	12-I	19-I	15-I
Control [b]	42	28	38	30	36	25	38	30	40	28	40	31

[a] L: Low activity = Mean of zone diameter ≤ 1/3 of mean zone diameter of control. I: Intermediate activity = Mean of zone diameter ≤ 2/3 of mean zone diameter of control. H: High activity = Mean of zone diameter > 2/3 of mean zone diameter of control.
[b] Cephalothin in the case of Gram-positive bacteria, chloramphencol in the case of Gram-negative bacteria and cycloheximide in the case of fungi. The concentration A is 2 mg/mL and B is 1 mg/mL.

It is known that the chelation tends to make the ligand acts as more powerful and potent bacterial agent. A possible explanation for this increasing the activity upon chelation is that in chelating complex, the positive charge of the metal is partially shared with donor atoms present on the ligands and there is an electron delocalization over the whole chelating ring. This, in turn, increases the lipoid layers of the bacterial membranes. Generally, it is suggested that the chelating complexes deactivate various cellular enzymes, which play a vital role in various metabolic pathways of Other factors such as solubility, conductivity and dipole moment, which affected by the presence of metal ions, which may also be possible reasons for increasing the biological activity of the metal complexes as compared to the ligand from which they are derived [57,58].

4. Conclusion

Copper(II), nickel(II), cobalt(II), zinc(II), cadmium(II), iron(III) and oxovanadium(IV) complexes of hydrazone, H_3L, ligand derived from the condensation *S*-methyldithiocarbazate and 4,6-diacetylresorcinol, in the molar ratio 1:1, has been synthesized. All the metal complexes were found to be dimmers. The structures of the ligand and its transition metal complexes were characterized by elemental analyses, spectral (infrared, electronic, mass, ^1H NMR and ESR) data and magnetic susceptibility, molar conductivity measurements and thermal gravimetric analysis (TGA). The structure of the ligand is dibasic tridentate with ONS sites. The metal complexes exhibit different geometrical arrangements such as square planar, tetrahedral, square pyramidal and octahedral arrangements. The ligand and its metal complexes were screened for its antimicrobial activity against *Staphylococcus aureus* and *Staphylococcus pyogenes* as Gram-positive bacteria, *Pseudomonas phaseolicola* and *Pseudomonas fluorescens* as Gram-negative bacteria and the fungi *Fusarium oxysporum* and *Aspergillus fumigatus*. Nickel(II) (2) and cobalt(II) (3) complexes showed high antimicrobial activities.

References

[1]. Casas, J. S.; Castellans, E. E.; Louce, M. D.; Ellena, J.; Sanchez, A.; Sordo, J.; Tabeada, C. *J. Inorg. Biochem.* **2006**, *100(11)*, 1858-1860.
[2]. Tain, Y. P.; Duan, C. Y.; Lu, Z. L.; You, X. Z.; Fun, H. K.; Kandasamy, S. *Polyhedron* **1996**, *15(13)*, 2263-2271.
[3]. Rodrigues, M. C.; Pinelli, S. J. *J. Inorg. Biochem.* **1995**, *58(3)*, 157-175.
[4]. Ferrari, M. B.; Fava, G. G.; Tarasconi, G.; Albertini, R.; Pinelli, S. J.; Starcich, R. *J. Inorg. Biochem.* **1994**, *53(1)*, 13-25.
[5]. Reper, E. S. *Coord. Chem. Rev.* **1985**, *61*, 115-148.
[6]. Padhye, S. B.; Kanffman, G. B. *Coord. Chem. Rev.* **1985**, *63*, 127-160.
[7]. Tofazzal, M.; Tarafder, H.; Ali, M. A.; Saravanan, N.; Weng, W. Y.; Kumar, S.; Tsafe, N. U.; Crouse, K. A. *Trans. Met. Chem.* **2000**, *25(3)*, 295-298.
[8]. Liu, Z. H.; Duan, C. Y.; Hu, J. *Inorg. Chem.* **1999**, *38(8)*, 1719-1724.
[9]. Liu, Z. H.; Yang, S. R.; Duan, C. Y.; You, X. Z. *Chem. Lett. Jpn.* **1999**, *10*, 1063-1069.
[10]. Tain, Y. P.; Duan, C. Y.; Zhao, C. U.; You, X. Z.; Mak, T. C. W.; Zhang, Z. *Inorg. Chem.* **1997**, *36(6)*, 1247-1252.
[11]. Taha, A.; Emara, A. A. A.; Mashaly, M. M.; Adly, O. M. I. *Spectrochim. Acta A* **2014**, *130*, 429-439.
[12]. Abu-Raabah, A.; Davies, G.; El-sayed, M. A.; El-Toukhy, A.; Shaikh, S. N.; Zubieta, J. *Inorg. Chim. Acta* **1992**, *193*, 43-56.
[13]. Chan, M. H. E.; Crouse, K. A.; Tahir, M. I. M.; Rosli, R.; Tsafe, N. U.; Cowley, A. R. *Polyhedron* **2008**, *27(4)*, 1141-1149.
[14]. Lobana, T. *Proc. Indian Acad. Sci. (Chem. Sci.)* **2000**, *112(3)*, 323-329.
[15]. Ali, M. A.; Nazimuddin, M.; Shaha, R.; Butcher, R. J.; Bryan, J. C. *Polyhedron* **1998**, *17(22)*, 3955-3961.
[16]. Hossain, M. E.; Alam, M. N.; Ali, M. A.; Nazimuddin, M.; Smith, F. E.; Hynes, R. C. *Polyhedron* **1996**, *150(5-6)*, 973-980.
[17]. West, D. X.; Liberta, A. E.; Padhye, S. B.; Chilate, R. C.; Sonawane, P. B.; Kumbhar, A. S.; Yerande, R. G. *Coord. Chem. Rev.* **1993**, *123*, 49-71.
[18]. Ali, M. A.; Haroon, C. M.; Nazimuddin, M.; Majumder, S. M. M. *Trans. Met. Chem.* **1992**, *17(2)*, 133-136.
[19]. Jain, S. K.; Garg, B. S.; Boon, Y. K.; Scovill, J. P.; Klayman, D. L. *Spectrochim. Acta* **1985**, *41(3)*, 407-413.
[20]. Campbell, M. J. *Coord. Chem. Rev.* **1975**, *15*, 279-319.
[21]. Chew, K. B.; Tarafder, M. T. H.; Crouse, K. A.; Ali, A. M.; Yamin, B. M.; Fun, H. K. *Polyhedron* **2004**, *23(8)*, 1385-1392.
[22]. Emara, A. A. A.; Abou-Hussen, A. A. A. *Spectrochim. Acta A* **2006**, *64(4)*, 1010-1024.
[23]. Emara, A. A. A.; Saleh, A. A.; Adly, O. M. I. *Spectrochim. Acta A* **2007**, *68(3)*, 592-604.
[24]. Flaschka, H. A. EDTA Titration, 2nd ed. Pergamon Press: New York, 1964, 81-86.
[25]. Vogel, A. I. Textbook of Quantitative Inorganic Analysis, 4th ed. Longman: London, 1978.
[26]. West, T. S. Complexometry with EDTA and Related Reagents, 3rd ed. DBH Ltd., Pools: New York, 1969.
[27]. Mabbs, F. E.; Machin, D. J. Magnitism and Transition Metal Complexes, Dover Publications: New York, 2008.
[28]. Gross, D. C.; De Vay, S. E. *Physiol. Plant Pathol.* **1977**, *11*, 13-28.
[29]. Bauer, A. W.; Kirby, W. W. M.; Sherris, J. C.; Turck, M. *Am. J. Clin. Pathol.* **1966**, *45(4)*, 493-496.
[30]. Ali, M. A.; Mirza, A. H.; Hamid, M. H. S. A.; Bernhardt, P. V. *Polyhedron* **2005**, 24 (3), 383-390.
[31]. Ali, M. A.; Mirza, A. H.; Ravoof, T. B. S. A.; Bernhardt, P. V. *Polyhedron* **2004**, *23(18)*, 2031-2036.
[32]. Ali, M. A.; Mirza, A. H.; Nazimuddin, M.; Ahmed, R.; Gahan, L. H.; Bernhardt, P. V. *Polyhedron* **2003**, *22(27)*, 3433-3438.
[33]. Emara, A. A. A.; El-sayed, B. A.; Ahmed, E. A. E. *Spectrochim. Acta A* **2007**, *69(3)*, 757-769.
[34]. Emara, A. A. A.; Seleem, H. S.; Madyan, A. M. *J. Coord. Chem.* **2009**, *62(15)*, 2569-2582.
[35]. Emara, A. A. A.; El-Sayed, B. A.; Ahmed, E. A. E. *Spectrochim. Acta A* **2008**, *69(3)*, 757-769.
[36]. Adly, O. M. I.; Emara, A. A. A. *Spectrochim. Acta A* **2014**, *132(1)*, 91-101.
[37]. Pretsch, E.; Seibl, J. Tables of Spectral Data for Structure Determination of Organic Compounds, Springer-Verlag: Berlin, 1983.
[38]. Abou-Husse,n A. A. A.; Emara, A. A. A. *J. Coord. Chem.* **2004**, *57(11)*, 973-987.

[39].   Emara, A. A. A. *Spectrochim. Acta A* **2010**, *77(1)*, 117-125.
[40].   Roy, S.; Mandal, T. N.; Barik, A. K.; Pal, S.; Gupta, S.; Hazra, A.; Butcher, R. J.; Hunter, A. D.; Zeller, M.; Kar, S. K. *Polyhedron* **2007**, *26(12)*, 2603-2611.
[41].   Khalil, S. M. E.; Emara, A. A. A. *J. Coord. Chem.* **2002**, *55(1)*, 17-32.
[42].   El-Sayed, B. A.; Abo Aly, M. M.; Emarly, A. A. A.; Khalily, S. M. E. *Vibr. Spectrosc.* **2002**, *30*, 93-100.
[43].   Adlly, O. M. I.; Tahly, A. *J. Mol. Str.* **2013**, *1038*, 250-259.
[44].   Nakamotly, K. Infrared Spectra of Inorganic and Coordination Compounds, 5th ed. John Willey & Sons: New York, 1997.
[45].   Adlly, O. M. I. *Spectrochim. Acta A* **2011**, *79(5)*, 1295-1303.
[46].   Greenwooly, N. N. Earnshaly, A.; Chemistry of the Elements, Pergamon Press: New York, 1984.
[47].   Kannappaly, R.; Tanalye, S.; Mutikainen, I.; Turpeinen, U.; Reedijk, J. *Inorg. Chem. Acta* **2005**, *358(2)*, 383-388.
[48].   Ali, M. A.; Bose, R. N. *Polyhedron* **1984**, *3(5)*, 517-522.
[49].   Goodgame, M.; Goodgame, D. M. L.; Cotton, F. A. *J. Am. Chem. Soc.* **1961**, *83(20)*, 4161-4167.
[50].   Cotton, F. A.; Wilkinson G. Advanced Inorganic Chemistry, A Comprehensive Text, 4th ed. John Wiley & Sons: New York, 1986.
[51].   Bailar, J. C.; Emeleus, H. J.; Nyholm, R.; Trotman-Dickenson, A. F. Comprehensive Inorganic Chemistry, Vol. 3. Pergamon Press: New York, 1975.
[52].   Lever, A. B. P. Inorganic Electronic Spectroscopy, 2nd ed. Elsevier: Amsterdam, 1997.
[53].   Emara, A. A. A.; Adly, O. M. I. *Trans. Met. Chem.* **2007**, *32(7)*, 889-901.
[54].   Geary, W. J. *Coord. Chem. Rev.* **1971**, *7(1)*, 81-122.
[55].   El-Ayaan, U.; Gabr, I. M. *Spectrochim. Acta A* **2007**, *67(1)*, 263-272.
[56].   Al-Ayaan, U.; El-Metwally, N. M.; Youssef, M. M.; El-Bialy, S. A. A. *Spectrochim. Acta A* **2007**, *68(5)*, 1278-1286.
[57].   Kaim, W. Schwederski B. Bioinorganic Chemistry: Inorganic Elements in the Chemistry of life, John Wiley & Sons: New York, 1994.
[58].   Ibrahim, M. A.; El-Mahdy, K. M. *Phosphorus, Sulfur and Silicon* **2009**, *184(11)*, 2945-2958.